Pergamon

Materials Research Bulletin 37 (2002) 1949–1960

Materials Research Bulletin

Microstructure characteristics for anorthite composite glass with nucleating agents of TiO_2 under non-isothermal crystallization

Chung-Lun Lo[a], Jenq-Gong Duh[a,*], Bi-Shiou Chiou[b], Wen-Hsi Lee[c]

[a]*Department of Materials Science and Engineering, National Tsing Hua University, Hsinchu, Taiwan 300, ROC*

[b]*Department of Electronics Engineering and Institute of Electronics, National Chiao Tung University, Hsinchu, Taiwan 300, ROC*

[c]*Phycomp Taiwan Ltd., Kaohsiung, Taiwan 811, ROC*

(Refereed)

Received 29 January 2002; accepted 24 June 2002

Abstract

The anorthite-based composite glass doped with TiO_2 and B_2O_3 was prepared by quenching of molten droplets. Phase development and crystals microstructure of glass were investigated under non-isothermal conditions. A glass transition temperature of 770°C and an exothermal peak around 870°C in the DTA trace was associated with anorthite crystallization ($CaAl_2Si_2O_8$). For glass specimens under nucleation and crystallization heat-treatment, the final predominant phase was identified as anorthite. Anorthite crystals show preferential nucleation at specific sites with rutile TiO_2 crystals precipitated from the glassy matrix and anorthite crystallization is governed by heterogeneous volume nucleation. The introduced TiO_2 plays the role of nucleating agents to reduce the crystallization temperature lower than 900°C for anorthite-based glass–ceramics. Chemical compositions could be related to the crystal microstructures on different characteristic regions. It was observed that the sintering aid of B_2O_3 neither reacted with nor dissolved in the anorthite or rutile TiO_2 crystals, and remained a glassy phase in the matrix. Occurrence of acicular precipitations was attributed to the orientation growth of TiO_2 crystals. Anorthite crystals were observed to grow with the forms of feathery-spherical particles, having a tendency to coalescence into a huge domain.

Keywords: A. Glasses; A. Ceramics; B. Crystal growth

* Corresponding author. Tel.: +886-3-5731164; fax. +886-3-5712686.
E-mail address: jgd@mse.nthu.edu.tw (J.-G. Duh).

0025-5408/02/$ – see front matter
PII: S0025-5408(02)00873-5

1. Introduction

Due to the high frequency transportation of signals for wide applications in the wireless communications and computer fields, a low dielectric constant, low temperature co-fired ceramic (LTCC) package was developed to achieve the requirements of high signal propagation speed, good reliability, and low cost [1,2]. In addition, properties such as dielectric constant ~5, appropriate thermal expansion coefficient and co-firability with other materials, make glass–ceramic systems compatible with high-performance multilayer ceramic substrates [3–5]. Anorthite ($CaO–Al_2O_3–2SiO_2$) based glass–ceramic system has been investigated and regarded as a potential material in LTCC substrates [6–8]. However, $CaO–Al_2O_3–SiO_2$ composite system glass are difficult to crystallize and they required the addition of nucleating agents for crystallization. TiO_2 is one of the most commonly used nucleating agents [9–11].

Fabrication technology of glass–ceramic substrates usually consists of the powder preparation and forming steps, followed by sintering and crystallization heat-treatments. If crystallization occurs before full densification, the viscosity among particles would increase significantly and retard sintering. Hence, it is essential to understand the crystallization behavior of the glass–ceramics system in order to fabricate reliable LTCC devices and then hopefully to control the final properties.

The crystallization characteristic is significantly affected by the composition of parent glass, including nucleating agents and the glass network former. Although the crystallization behavior of anorthite in $CaO–Al_2O_3–SiO_2$ glass has been reported [12–15], little attention has been paid to the microstructure development during nucleation and crystallization processing. The aim of the present study was to evaluate the microstructure characteristics of non-isothermal crystallization in the anorthite-based glass ($CaO–Al_2O_3–2SiO_2–TiO_2–B_2O_3$). The investigations in nucleation and crystallization were conducted using differential thermal analysis (DTA), high-temperature X-ray diffractometry (HTXRD), and scanning electron microscopy (SEM) techniques. In addition, the non-isothermal crystallization mechanism was discussed with respect to the chemical composition analysis and crystal morphology observation.

2. Experimental

The compositions of the glasses studied were based on the anorthite ($CaAl_2Si_2O_8$) composition. It was derived from the technical grade powders of silicon oxide, calcium oxide, and aluminum oxide with the near stoichiometry of $CaO:Al_2O_3:SiO_2 = 1:1:2$, along with 18 wt.% TiO_2 and 10 wt.% B_2O_3. TiO_2, used as a bulk-nucleating agent in silica-based glass, is miscible in the glassy network, at high temperatures [16,17]. B_2O_3 was chosen as a sintering aid for lowering the melting temperature. A glass batch of homogeneous mixture was prepared by ball milling and then melted in a Pt crucible at 1650°C for 10 h in an electric furnace to achieve a homogenized melt. To prepare glass bulk samples, the melt was cast into a steel mold

and then slowly cooled from 600°C to room temperature. Glass pieces were cut into a size of 10 mm × 10 mm × 5 mm and then polished using SiC emery paper and Al_2O_3 polishing medium to obtain a clean and smooth surface. Crystallization heat-treatment experiments were carried out at selected temperatures in the range of 800–1000°C.

A differential thermal analyzer (DTA1600, DuPont, USA) was used to study the crystallization behavior and to determine the glass transition temperature, T_g. The DTA instrument was previously calibrated by using Al, Ag, and Zn specimens, which have accurate melting temperatures. The DTA analysis was performed under a flowing atmosphere of dry air (50 cm^3/min). The glass was then heated at a rate of 5°C/min up to 1000°C with a reference material of α-alumina powders. Identification of the high-temperature phase of the specimens was performed by HTXRD (X'pert PW3040/00, Philips, Holland) with a wavelength of Cu Kα ($\lambda = 1.5406$ Å). A small amount of the powders were mounted on a Pt stage-heating element. A R-type thermocouple spot-welded to the bottom of the stage was used for temperature measurement. XRD patterns were recorded at different temperatures in the rage between 860 and 950°C with an increment of 5°C for each run. Short scanning was performed from 20 to 40°(2θ) at a scan rate of 5°/min.

The morphology and microstructure of the crystallized glass pieces were examined using optical microscopy and SEM (JEOL 840A, Japan). Electron probe microscopy (EPMA; JEOL JXA-8800M, Japan) was also used to analyze the composition of the glass and the crystalline phase.

3. Results and discussion

DTA was conducted on the as-fabricated glass. Fig. 1 shows the respective DTA trace of anorthite-based glass under a non-isothermal heat-treatment at a constant heating rate of 5°/min. According to El-Shennawi et al. [18], the endothermic trend in DTA trace for a glass material can be determined as the transition temperature of glass (T_g), which is believed to be caused by an increase in heat capacity attributed to the transformation of the glass structure [19]. For this reason, T_g can be measured using DTA and will appear as an endothermic trend with increasing temperature, as shown in Fig. 1. The convention for determining the glass transition temperature is to extend the straight-line portions of the baseline and the linear portion of the upward slope, marking their intersection. It is observed that anorthite-based glass powders initially go through a transition temperature of glass around 770°C (T_g), and then one exothermic transformation apparently occurs (crystallization peak temperature, $T_p = 868$°C), corresponding to subsequent crystallization from the glass matrix.

On the basis of DTA results, HTXRD were carried out to verify the crystal phases in the glass matrix. Fig. 2 presents the corresponding HTXRD patterns for glass at various temperatures. At temperatures slightly higher than T_g, no significant peaks were revealed, indicating amorphous glass matrix in the as-fabricated state. Minor peaks of titanium oxide and anorthite were initially observed at temperatures from

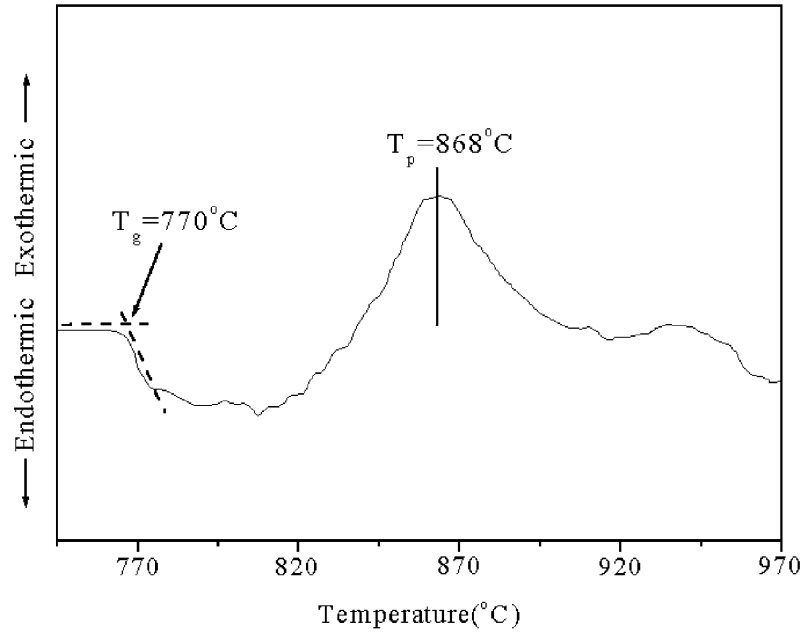

Fig. 1. DTA curve in the anorthite-based glass crystallized at a temperature rate of 5°/min.

870 to 900°C. However, at higher temperatures, the rutile TiO_2 peaks disappear, while those for the anorthite crystal became sharper and more significant. Therefore, the crystallization process takes place in the glass matrix at the temperature above the peak temperature, T_p (870°C) and the major phase is anorthite. As expected, the major

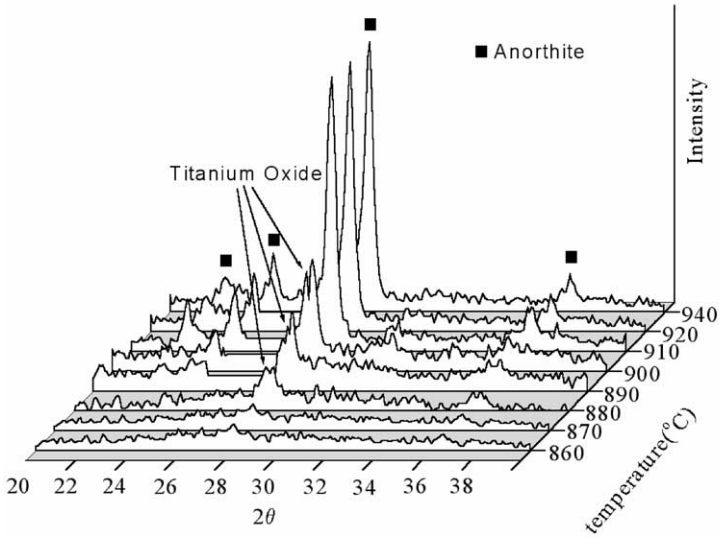

Fig. 2. HTXRD patterns of the anorthite-based glass heat-treated at different temperatures.

exothermal peak, T_p, in DTA curve (Fig. 1) was correlated to the crystallization of anorthite from the glass matrix. By combining DTA and HTXRD results, it is concluded that the crystallization of anorthite from anorthite-based glass nucleated with TiO_2 starts around 830°C and terminates at 920°C. For glass–ceramic materials in LTCC technology, the lower crystallization temperature (<950°C) is a restrictive requirement to co-fire with highly conductive metals, such as copper and silver, below their melting temperature.

During the fabrication of LTCC substrates, the role of the sintering process is expected by the glassy viscous flow to achieve a fully densified product. In this study, anorthite-based glass nucleated with TiO_2 has a glass transition temperature of 770°C and crystallization of the glass occurred at low temperature up to 830°C by the formation of anorthite phase in glass. On the other hand, a temperature range between 770 and 830°C can be attributed to sintering, while a temperature above 830°C is a step toward crystallization.

To investigate the morphology of the resultant microstructure after crystallization, optical microscopy and SEM investigations were conducted on the bulk specimen of glass heated to 870°C ($\sim T_p$) followed by air quenching. As crystals form in the glass matrix, the devitrification was clearly observed. The amorphous glassy phase is still transparent, yet the crystal becomes devitrified so that the morphology difference between them can be easily observed in an OM micrograph, as shown in Fig. 3(a). Crystals, which have grown to have spherical-feathery shapes, have an approximate size of 100 μm in diameter. It should be mentioned that the crystallization occurs not only on the surface, but also in the bulk of the glass, which indicates that the bulk crystallization is also predominant in the glass sample. Fig. 3(b) is the corresponding SEM micrograph of the anorthite-based sample taken in the back-scattered electron imaging (BEI) mode. Crystal morphologies in the glass exhibited different shapes of star-like, feathery, and acicular growth. The chemical composition of region A (center of the feathery grown crystal), region B (acicular markings), and region C (glassy matrix) were evaluated by EPMA. Table 1 lists the summarized results of the quantitative analysis. Ten different locations on the glassy matrix [region C in Fig. 3(b)] were measured and the average compositions were 6.33 ± 0.06 at.% Ca, 12.34 ± 0.30 at.% Al, 12.82 ± 0.27 at.% Si, 3.74 ± 0.22 at.% Ti, 60.00 ± 1.00 at.% O, 4.77 ± 0.32 at.% B, which is similar to the composition of initially as-fabricated anorthite glass. Region B in Fig. 3(b) contained only Ti and O signals, exhibiting an atomic ratio of Ti:O as 1:2. Thus, combined with the XRD results, it is evident that TiO_2 phase is present and developed with the shape of acicular growth in an anorthite-based glass matrix. The center of the spherical particles indexed as A in Fig. 3(b) contained 6.71 ± 0.16 at.% Ca, 13.27 ± 0.41 at.% Al, 13.56 ± 0.74 at.% Si, 4.49 ± 0.31 at.% Ti, 61.97 ± 1.32 at.% O, similar to stoichiometric anorthite ($CaAl_2Si_2O_8$) composition with TiO_2 ($\sim$4 mol%) in the crystallized anorthite phase. It appears that boron would neither react with nor dissolve in the anorthite phase, since the boron signal was not detected in Region A. Such well-crystallized anorthite crystals (Region A) were enclosed with the centro-symmertric TiO_2 acicular crystals and surrounded by the spherical region[Region E in Fig. 3(b)]. The Region E can be considered as the transition zone for anorthite crystals (Region A)

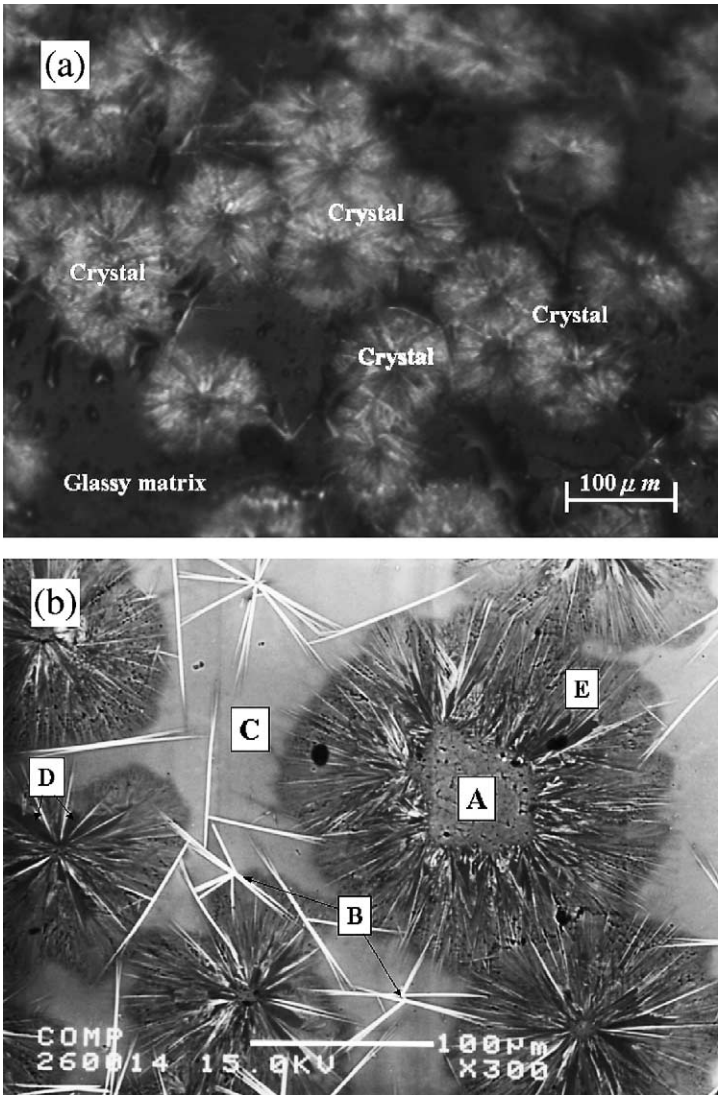

Fig. 3. Optical (a) and BEI (b) micrographs of the anorthite glass heated to 870°C followed by air quenching.

grown into the amorphous glassy matrix. The average atomic ratio of Region E was measured as 7.31 ± 0.64 at.% Ca, 14.03 ± 1.23 at.% Al, 14.82 ± 1.77 at.% Si, 4.52 ± 0.72 at.% Ti, 58.05 ± 1.93 at.% O, and 1.27 ± 1.06 at.% B. The quantitative result for this transition region exhibiting a larger deviation for Ti (±16%) and B (±83%) indicates that both atoms are randomly dissolved in the transition zone. It is believed that the transition region is not the equilibrium phase ($CaAl_2Si_2O_8$), but a metastable product. It is evident that the glass–crystal interfaces are resulted from the different amount of boron atoms between them. Another specific region was also observed in the microstructure of anorthite crystals. From the magnified BEI

Table 1
List of chemical compositions (at.%) on different indexed region in Fig. 3(b)

Indexed region	Ca	Al	Si	Ti	O	B	Remark
A	6.71 ± 0.16	13.27 ± 0.41	13.56 ± 0.74	4.49 ± 0.31	61.97 ± 1.32	–	$CaAl_2Si_2O_8 + TiO_2$
B	–	–	–	33.50 ± 0.62	66.50 ± 1.20	–	TiO_2
C	6.33 ± 0.06	12.34 ± 0.30	12.82 ± 0.27	3.74 ± 0.22	60.00 ± 1.00	4.77 ± 0.32	Amorphous glass
D	6.67 ± 0.24	13.89 ± 0.84	14.21 ± 0.98	1.23 ± 0.51	63.81 ± 1.24	0.25 ± 0.15	Depletion zone of Ti
E	7.31 ± 0.64	14.03 ± 1.23	14.82 ± 1.77	4.52 ± 0.72	58.05 ± 1.93	1.27 ± 1.06	Transition zone

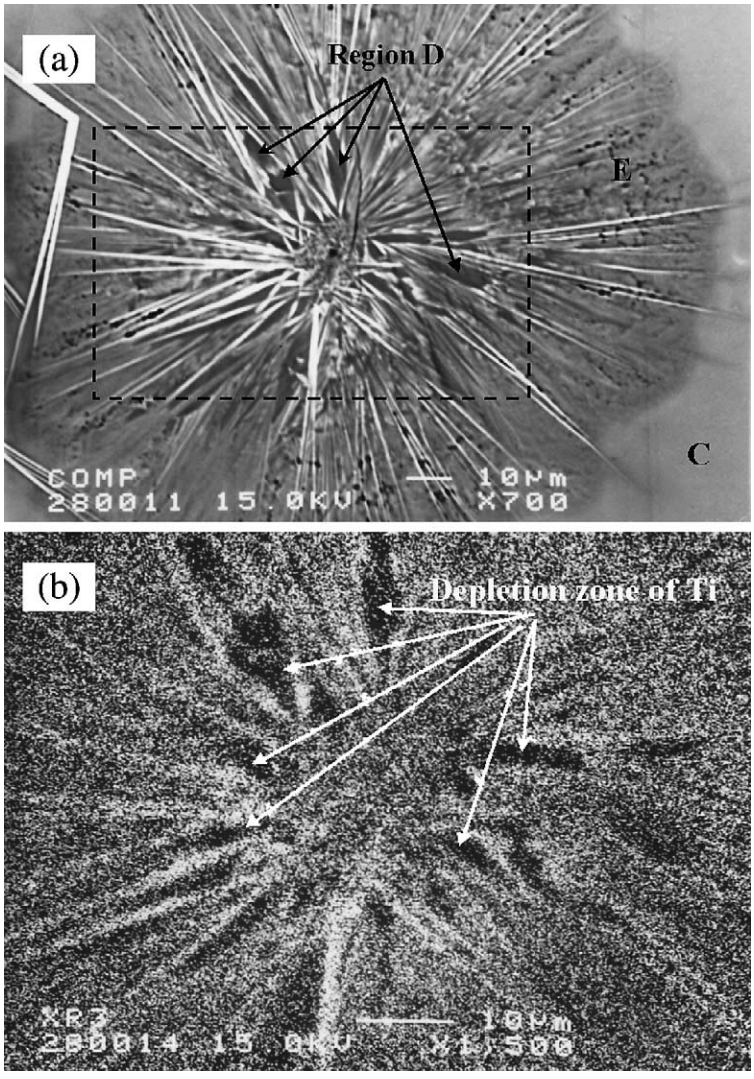

Fig. 4. BEI micrograph (a) and X-ray mapping (b) of Ti for individual crystals in the glassy matrix.

micrograph on a single particle of anorthite crystal as shown in Fig. 4(a), regions with darker color were around the centro-region and interlaced with acicular TiO_2 crystals (indexed as D). These regions exhibited a depletion of Ti, as indicated in the X-ray mapping of Ti shown in Fig. 4(b). The depletion region contained 1.23 ± 0.51 at.% Ti and 0.25 ± 0.15 at.% B, which are less than those of Region E. The presence of this depletion zone may be attributed to the precipitation of TiO_2 crystals in the early stage for crystallization. As the nucleating agent of TiO_2 is precipitated in the glassy matrix to form a centro-symmetrically acicular geometry, the local enrichment of Ti at the acicular TiO_2 (Ti: 33 and 67 at.%) would tend to consume the surrounding Ti atoms, resulting in a depletion zone locally, particularly when the acicular TiO_2 crystals

are rather close. As shown in Fig. 4(b), the local depletion zone of Ti occurs at the near-center area, where the distance is the shortest between the two detached acicular rutile TiO_2.

From the DTA data, it is expected that there was no visible crystallization below the temperature of 830°C. The devitrification also was not detected by OM observation on the glass sample. When the sample was heat-treated above 830°C, a series of BEI micrographs of the glass bulk were taken after heat-treating at different temperatures followed by quenching to room temperature, as shown in Fig. 5. At 840°C, a smaller amount of acicular crystal (~15 μm in length) precipitation from the glassy matrix was observed, as indicated in Fig. 5(a). Those acicular-shaped and star-like crystals are composed of TiO_2 phase surrounded by the amorphous glassy matrix in anorthite-based glass. When the glass specimen was heat-treated up to 870°C [$\sim T_p$ in DTA curve of Fig. 1)], anorthite crystals rapidly grew on the base of the as-precipitated rutile TiO_2 crystals. As shown in Fig. 5(b), the anorthite crystals grew up from the central sites of the aggregated TiO_2 crystals into a glassy matrix to form a feathery, star-like, and spherical particles, which included the transition zone surrounding the anorthite crystals. These particles contained anorthite and TiO_2 crystals, which exhibit an approximate diameter of 100 μm, with two growing spherical particles encountered. At higher temperatures, the particles may experience coarsening because the difference in particle size represents a variation in the chemical activity from particle to particle. The driving force was attributed to the reduction of the interfacial free energy. An abnormally large domain based on anorthite crystals, originating from several spherical growing particles, appears in the glassy matrix as shown in Fig. 5(c).

Fig. 6(a) and (b) shows the XRD patterns for the quenched glass specimens heat-treated to 870 and 920°C, respectively, at the rate of 5°/min followed by quenching in air. On the initial stage of crystallization from amorphous glassy matrix, the TiO_2 crystal exhibited a strong crystallographic orientation along (1 1 0) planes and small amounts of anorthite crystals were detected. It is argued that diffusion is probably rate-determining at a relative lower temperature. Consequently, acicular precipitates form, having crystallographic orientation with the matrix. Nevertheless, the rate of growth is limited, and results in star-like crystals. However, at higher temperatures, there is a tendency for a spherical particle (containing $CaAl_2Si_2O_8$ and TiO_2 crystals) in Figs. 3 and 5(b) to develop, in which the total surface energy is minimum and the strain energy may be relieved by the viscous flow of the glassy matrix. With the higher temperature, anorthite crystals dominate the main phase in the crystallized glass, which is evident in the XRD pattern shown in Fig. 6(b).

After a series of investigations into the crystal morphology and microstructural development of the non-isothermal crystallization in anorthite-based glass, it can be concluded that the anorthite crystals show preferential nucleation at specific sites on the base of rutile TiO_2 crystals, which indicates that anorthite crystallization is governed by heterogeneous nucleation. On the other hand, the introduction of TiO_2 plays the role of a nucleating agent to reduce the crystallization temperature to less than 900°C for anorthite-based glass–ceramics, which is beneficial for the application

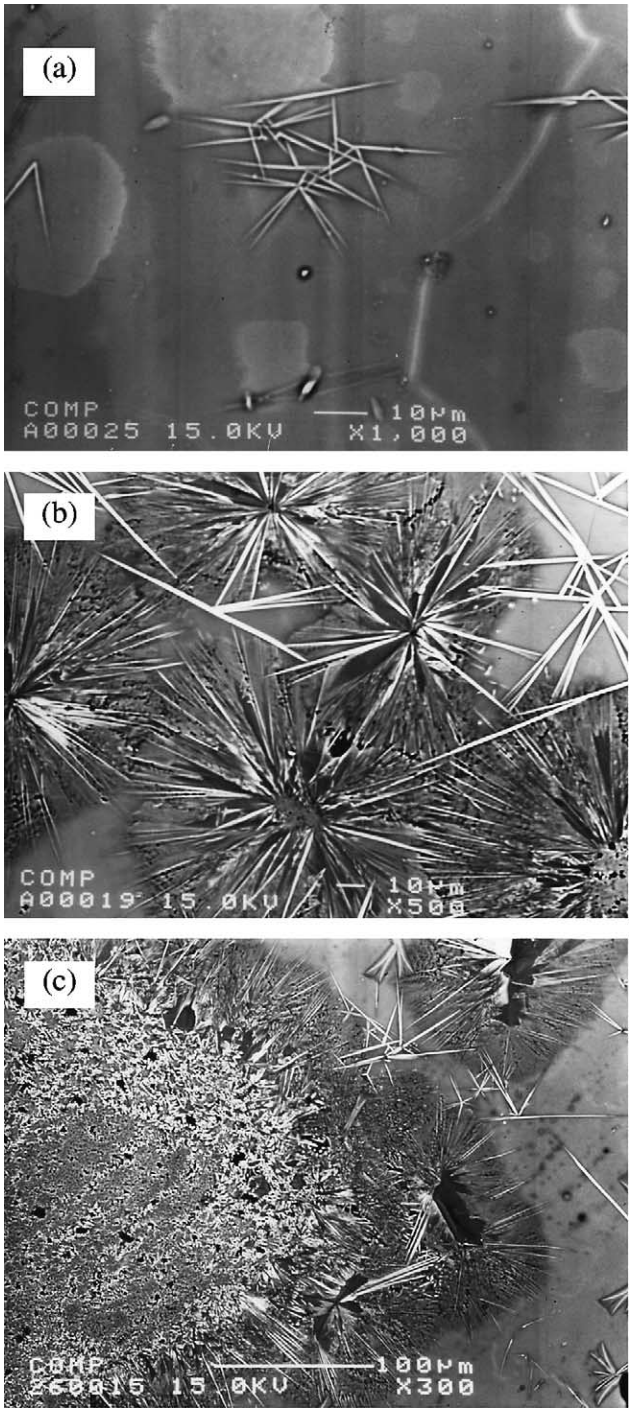

Fig. 5. BEI micrographs of the anorthite-based glass after heat-treating at various temperatures of 840°C (a), 870°C (b), and 900°C (c) followed by quenching in air.

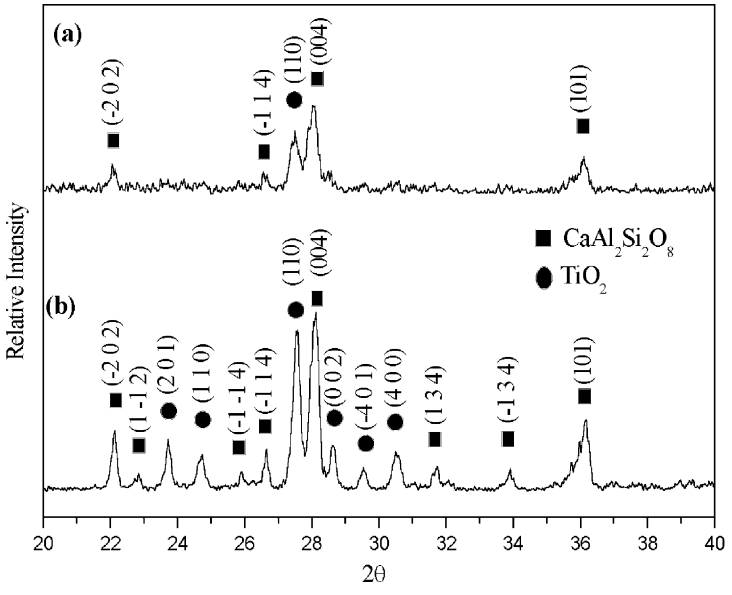

Fig. 6. X-ray diffraction patterns of the anorthite-based glass heated to 870°C (a) and 920°C (b) at a rate of 5°C/min to various temperatures followed by quenching in air.

in LTCC. Besides, the sintering aid of boron oxide would not react with the anorthite and rutile TiO_2 crystals, and it would remain a glassy phase in the matrix. As a result, for the green body sintering process in a glass–ceramic LTCC substrate, the volume heterogeneous nucleation within particles may inhibit the surface crystallization and enhance densification via glassy viscosity flow at the temperatures above T_g. The remaining glassy B_2O_3 may also act to reduce the viscosity of the uncrystallized matrix.

4. Conclusions

1. The crystallization of anorthite from $CaO–Al_2O_3–SiO_2–TiO_2–B_2O_3$ composite glass exhibited a glass transition temperature of 770°C, and crystallization of the glass occurred at temperatures as low as 830°C via the formation of anorthite phase in glass.
2. The orientation growth of rutile TiO_2 crystals resulted in acicular precipitations. Anorthite crystals were observed to grow with the forms of feathery-spherical particles initially and then exhibiting a tendency of gathering into a huge domain.
3. The introduction of TiO_2 in anorthite-composed glass provided nucleation sites for the growth of anorthite crystals at temperature below 900°C. B_2O_3, acted as the sintering aid, yet it would neither react with nor dissolve in the anorthite or rutile crystals, and remained as a glassy phase in the matrix.

Acknowledgments

This work is supported by the Philips Electronics Building Elements Industrial (Taiwan) Ltd. under contract no. C89054. Partial support from the National Science Council, under the contract #NSC-89-2216-E009-038, is also appreciated.

References

[1] A.H. Kumar, P.W. McMillan, R.R. Tummala, Glass-ceramic structures and sintered mulyilayer substrates there of with circuit patterns of gold silver or copper, US Patent No. 4,301,324 (17 Nov. 1981).
[2] Y.K. Shimade, U.M. Suzuki, H. Takamizowa, IEEE trans. components, Hybrids Manuf. Technol. CHMT-6 (4) (1983) 382.
[3] R.R. Tummala, Ceramic and glass-ceramic packaging in the 1990s, J. Am. Ceram. Soc. 74 (1991) 895.
[4] R.R. Tummala, S. Ahmed, IEEE trans. components, Hybrids Manuf. Technol. 15 (4) (1992) 426.
[5] D.M. Mattox, S.R. Gurkovich, J.A. Olenick, K.M. Mason, Ceram. Eng. Sci. Proc. 9 (1988) 1567.
[6] Corning corporation, Anorthite glass-ceramics, US Patent No. 4,187,115 (5 Feb. 1980).
[7] J.A. Topping, Ceram. Bull. 56 (1977) 574.
[8] NEC corporation, Mutlilayer glass ceramic substrate and method of fabricating, US Patent No. 5,506,058 (9 Apr. 1996).
[9] N.P. Padture, H.M. Chan, J. Mater. Res. 7 (1) (1992) 170.
[10] H.C. Park, S.H. Lee, M.M. Son, H.S. Lee, I. Yasui, J. Mater. Sci. 31 (1996) 4249.
[11] C. Leonelli, T. Manfredini, M. Paganelli, P. Pozzi, G.C. Pellacani, J. Mater. Sci. 26 (1991) 5041.
[12] B. Ryu, I. Yasui, J. Mater. Sci. 29 (1994) 3323.
[13] Y. Kobayashi, E. Kato, J. Am. Ceram. Soc. 77 (3) (1994) 833.
[14] R.G. Duan, K.M. Lian, J. Mater. Proc. Tech. 75 (1998) 235.
[15] E. Wittman, E.D. Zanotto, J. Non-Cryst. Solids 271 (2000) 94.
[16] W. Vogel, Glass Chemistry, Springer, Berlin, 1994.
[17] P.W. McMillan, Glass-Ceramics, Academic Press, London, 1964.
[18] A.W.A. El-Shennawi, M.M. Morsi, G.A. Khater, S.A.M. Abdelhamid, J. Thermochim. Acta. 51 (1998) 553.
[19] K. Watanbe, E.A. Giess, J. Non-Cryst. Solids 169 (1994) 306.